Electrochemical Deposition of a New n-Doping Polymer Based on Bis(thienyl)isopyrazole

David L. Witker,[a] Sean O. Clancy,[b] David J. Irvin,
John D. Stenger-Smith, and Jennifer A. Irvin*,[z]

Chemistry Division, Naval Air Warfare Center Weapons Division, China Lake, California 93555, USA

A novel donor-acceptor polymer based on thiophene and isopyrazole has been prepared for use in n-doping applications. Nonpolymerizable monomer radical cations appear to be the predominant oxidation product, resulting in a need for extended cycling to produce adequate quantities of polymer for characterization. The electrochemical behavior of the polymer films produced is strongly dependent upon the conditions applied during electrodeposition and on the solvent used during cycling of the films. Cycling to reductive potentials during oxidative polymerization in acetonitrile was necessary to produce a polymer film capable of n-doping, likely resulting from a need to establish pathways for cation migration. The neutral polymer undergoes oxidation to the p-doped form at ca. 2000 mV vs Ag/Ag$^+$ in propylene carbonate and reduces back to neutral at ca. 0 mV. Conversion of the neutral polymer to its n-doped form involves reductions at -700 and -1300 mV, with reoxidation at -800 and -200 mV to return to the neutral form of the polymer.
© 2007 The Electrochemical Society. [DOI: 10.1149/1.2436991] All rights reserved.

Electroactive polymers can generally be switched between two or more stable oxidation states, giving rise to changes in properties including conductivity, color, and volume. Electroactive polymers which have been oxidized from a neutral state are said to be p-doped, by analogy to semiconductor terminology. Likewise, polymers that have been reduced from a neutral state are described as being n-doped. Owing to the inherent stability of carbocations, p-dopable materials are quite well known and have been thoroughly documented.[1-3] On the other hand, no conjugated polymers have been found to be electrochemically stable during n-doping.[4-6] The instability of n-doping conjugated polymers is most likely due to the highly reactive nature of carbanions.[4] However, stable n-doping materials are indeed quite desirable, as they may find utility in a number of applications, including batteries and supercapacitors.[7]

One approach being explored to obtain stable n-doping polymers is the synthesis of donor-acceptor materials.[8-11] In this type of system, the polymer HOMO is much like the relatively high-energy HOMO of the donor material, while the polymer LUMO is energetically similar to the relatively low-energy LUMO of the acceptor. This type of electronic architecture leads to a small HOMO-LUMO gap in the polymers and consequently a low-lying polymer LUMO suitable for accepting charge.

The electron-poor functionality of the acceptor groups can be accomplished in one of two ways. In the most common approach, electron-withdrawing substituents such as nitro- or fluorogroups are incorporated pendant to the main chain of the polymer.[9,10] While this method can yield electron-deficient monomer units and ultimately electron-deficient polymers, it is likely that the substituents act as charge traps, hindering electron mobility.

Electron mobility might be improved by incorporation of functional groups that are themselves intrinsically electron-deficient without the aid of pendant groups, such as the high nitrogen heterocycles. Empirically, the higher the electron affinity of the polymer, the more stable the polymer will be in the n-doped state.[12] In general, as the number of imine-type nitrogens replacing carbon in a given aromatic ring increases, so too does that ring's electron affinity.[13] Incorporation of these high nitrogen heterocycles into conjugated polymers should result in n-dopable polymers with good electron mobility. Limited research into this type of donor-acceptor polymer can be found in the literature.[8,11]

Here we report on a new donor-acceptor polymer for use in n-doping applications. As the electron-rich portion of the polymer we have chosen thiophene units, while we have chosen the isopyrazole ring as the electron deficient portion. The isopyrazole group should prove advantageous due to its high electron affinity[13] and ease of functionalization.

Experimental

Dimethyl malonyl chloride, *n*-butyllithium (2.5 M in hexanes), zinc chloride (1.0 M in diethyl ether), 2-bromothiophene, palladium(II) chloride, hexanes, methanol, toluene, calcium hydride, calcium oxide, and hydrazine hydrate were purchased from Aldrich and used as received. Triphenyl phosphine was purchased from Aldrich and sublimed prior to use. Sodium bicarbonate and sodium sulfate (dibasic) were purchased from Polarchem and used as received. Acetone was purchased from JT Baker and used as received. Diethyl ether was purchased from VWR Scientific and used as received. Chromatographic grade silica gel (100–200 mesh) was purchased from Fisher Scientific and used as received. Pd(PPh$_3$)$_4$ was synthesized by reduction of PdCl$_2$ with hydrazine in the presence of PPh$_3$.

All electrochemical experiments were performed in a nitrogen atmosphere dry box using a Parstat model 2237 potentiostat. Acetonitrile was dried by distillation from calcium hydride at atmospheric pressure. Propylene carbonate was dried by distillation from calcium oxide at atmospheric pressure. Tetramethylammonium tetrafluoroborate (TMABF$_4$, purchased from Aldrich) was recrystallized twice from methanol/water. The electrolyte was then dried in a vacuum oven at 110°C for twenty-four hours before use. Electropolymerizations were conducted with a 10 mM solution of monomer in 100 mM TMABF$_4$/acetonitrile. The working, auxiliary, and reference electrodes were a platinum button (area = 0.02 cm^2), a platinum flag, and a nonaqueous Ag/Ag$^+$ reference electrode (consisting of silver wire in a solution of 0.1 M TMABF$_4$ and 10^{-2} M AgNO$_3$ in acetonitrile), respectively. The potential of the Ag/Ag$^+$ reference electrode was calibrated using the ferrocene/ferrocinium couple. The reduction potential of the couple was found to be 97 mV vs the reference electrode. All potentials reported herein are relative to the Ag/Ag$^+$ reference electrode. Cycling of the polymer films was accomplished using monomer-free 100 mM TMABF$_4$ in propylene carbonate as the electrolyte system.

1,3-Dithien-2-yl-2,2-dimethylpropane-1,3-dione (DMDTPy).— 2-bromothiophene (12.4 mL, 32.0 mmol) was added to 500 mL dry diethyl ether under nitrogen. Then *n*-butyl lithium (2.5 M in hexanes, 50.8 mL, 127.2 mmol) was added and the mixture was stirred for sixty minutes. After this time, ZnCl$_2$ (1.0 M in diethyl ether, 127.2 mL, 127.2 mmol) was added slowly, giving a white precipitate. Next, the reaction mixture was allowed to slowly warm to room
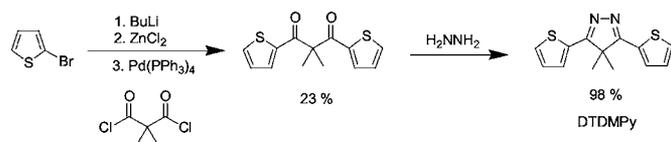
Figure 1. Synthesis of 3,5-dithien-2-yl-4,4-dimethylpyrazole (DTDMPy).

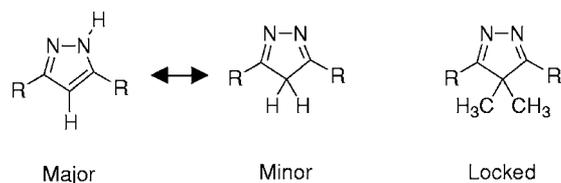**Figure 2.** Resonance structures of a 3,4-substituted pyrazole showing a conjugation-breaking major tautomer structure and a minor structure giving complete conjugation; 4,4-dimethyl analog with a "locked" electronic structure.

temperature and was then heated at reflux for four hours. Following the reflux period, the reaction mixture was cooled to room temperature and Pd(PPh$_3$)$_4$ (1.85 g, 1.6 mmol) was added followed by the slow addition of dimethyl malonyl chloride (2.0 mL, 15.1 mmol). After completion of the additions, the reaction mixture was brought to reflux and stirred overnight.

After this time, the reaction mixture was poured into 500 mL saturated aqueous sodium bicarbonate. The two-phase mixture was filtered and separated. The organic phase was washed with brine and dried over sodium sulfate. The solvent was removed by rotary evaporation under reduced pressure without heating to give a pale orange solid. This solid was dissolved in a minimal amount of acetone and passed under vacuum through a short plug of silica gel using hexanes as the eluent. The solvent was removed by rotary evaporation with heating under reduced pressure to yield a pale yellow solid. This material was recrystallized from hexanes to give pale yellow needles. Yield 3.7 g, 23%. Mp: 159–162°C. ^{1}H NMR (CDCl$_3$) δ 7.54 (m, 4 H), 6.99 (dd, 2 H, J = 5.0, 4.0 Hz), 1.69 (s, 6 H). IR (KBr pellet, cm^{-1}): 3114.4, 3099.0, 2994.1, 2932.5, 1663.3, 1636.2, 1512.9, 1461.1, 1408.0, 1352.6, 1268.8, 1254.0, 1241.7, 1172.6, 1054.3, 965.5, 903.9, 852.1, 825.0, 748.5, 726.3.

3,5-Dithien-2-yl-4,4-dimethylpyrazole.— DMDTPy (1.25 g, 4.7 mmol) and anhydrous hydrazine (1.5 mL, 47 mmol) were combined in 100 mL toluene under nitrogen. The resulting solution was then heated at reflux for eighteen hours. After this time, the solvent was removed by rotary evaporation with heating under reduced pressure, and the bright orange solid remaining was collected and dried in vacuo. Yield 1.21 g, 98%. MP: 153–156°C. ^{1}H NMR (CDCl$_3$) δ 7.65 (dd, 2 H, J = 3.8, 1.0 Hz), 7.52 (dd, 2 H, J = 5.0, 1.0 Hz), 7.17 (dd, J = 5.1, 3.8 Hz), 1.70 (s, 6 H). ^{13}C NMR (CD$_2$Cl$_2$) δ 174.5, 133.9, 130.1, 129.0, 128.6, 59.3, 24.5. IR (KBr pellet, cm^{-1}): 3095.9, 2988.0, 2972.6, 2929.4, 2861.5, 1538.2, 1492.0, 1455.0, 1430.3, 1226.7, 1057.1, 850.4, 835.0, 720.8, 699.3. Elemental analysis: 58.61% C, 4.89% H, 10.76% N.

Results and Discussion

The synthesis of the monomer (DTDMPy) used in this work was accomplished using a relatively simple two-step procedure (Fig. 1). The first step entailed coupling of a thienylzinc reagent to dimethyl malonyl chloride using a palladium (0) catalyst. Although the poor diethyl ether solubility of the thienylzinc reagent likely contributed heavily to the low yields (23%) attained, the target was easily separated from side products by chromatography and then further purified by recrystallization from hexanes. When tetrahydrofuran was used as the solvent, the thienylzinc reagent was more soluble than in diethyl ether, but the material isolated after the reaction was a complex mixture that could not be separated. Infrared spectroscopy of the product showed a sharp, prominent absorbance at 1636 cm^{-1}, indicating that conjugated carbonyl groups were present; ^{1}H NMR of the product was consistent with the proposed structure.

The second step of the process, a ring-closing reaction with excess hydrazine to afford the pyrazole ring, was accomplished in nearly quantitative yield. This result indicates that the ring-closing step is much more kinetically favorable than is the addition of a second hydrazine to the dione. Infrared spectroscopy of this product showed no trace of the carbonyl vibration observed with the precursor, indicating that the conversion to pyrazole was complete. ^{1}H NMR, ^{13}C NMR, and elemental analysis of the product are all con-

sistent with the proposed structure. It is expected that this general reaction scheme will be applicable to other ring systems besides thiophene to give a wide array of diarylpyrazole derivatives, including those that are more electron-deficient than DTDMPy.

A vital consideration in monomer design was the substitution pattern of the pyrazole ring. In order to produce a monomer suitable for electroactive polymers, it is necessary to quaternize the carbon at the 4-position of the pyrazole ring. An unsubstituted pyrazole in this situation has as its major tautomer a protonated amine as part of the ring (Fig. 2). This type of electronic structure of course serves as a conjugation break. In order to exclude this tautomer, the carbon at the 4-position must be fully substituted. Dimethyl malonyl chloride, a commercially available building block, was used with the anticipation that the methyl groups would give rise to the correct electronic structure for a fully conjugated polymer. In addition, after electropolymerization, the methyl substituents were not expected to impart much solubility to the polymer.

During electropolymerization in propylene carbonate, a yellow-orange material could be seen moving away from the electrode. This could possibly be attributed to soluble oligomers diffusing away from the electrode into solution. No such behavior was noticed during polymerization in acetonitrile. However, better defined n-doping processes were observed during cycling in propylene carbonate than in acetonitrile. Therefore the results reported herein are based on electropolymerization of 10 mM monomer using 100 mM TMABF$_4$ in acetonitrile and cycling in monomer-free 100 mM TMABF$_4$ in propylene carbonate.

Initial electropolymerizations of DTDMPy were accomplished by cycling the potential applied to a platinum button repeatedly between 0 and 2000 mV vs Ag/Ag$^+$. All further electrochemical potentials are reported with respect to this reference. It was necessary to cycle the potential for two hours to produce a film thick enough for electrochemical characterization. This result is in contrast to those reported for more electron-rich monomers, such as thiophene derivatives that can be deposited in a relatively short time.[14] The voltammograms generated during electropolymerization show monomer oxidation onset at ca. 1200 mV and peak at ca. 1800 mV along with a slowly growing current response centered at about 1200 mV that can be attributed to polymer oxidation (Fig. 3). Interestingly, there appears to be no corresponding reduction for the polymer. Instead, reductions at more positive potentials are present. This reduction most likely is due to monomer reduction, suggesting that a large portion of the monomer is first oxidized and then reduced without coupling to form polymer. The polymer reduction response is likely obscured by the more intense monomer reduction current.

The limited coupling upon monomer oxidation can best be explained by considering the effect of the pyrazole ring on the resonance forms of the monomer. As is the case with a more traditional monomer like terthiophene, oxidation gives a radical cation. The radical may be located at the 5-position of a terminal thiophene, thus leading ultimately to 2,5-linked polythiophene (Fig. 4). However, if the radical migrates through the monomer, it may be located on the 3- or 4-position of one of the thiophene rings. This electronic arrangement leads to the often-undesirable irregularly linked polymer chains that are not fully conjugated. By analogy, DTDMPy may be
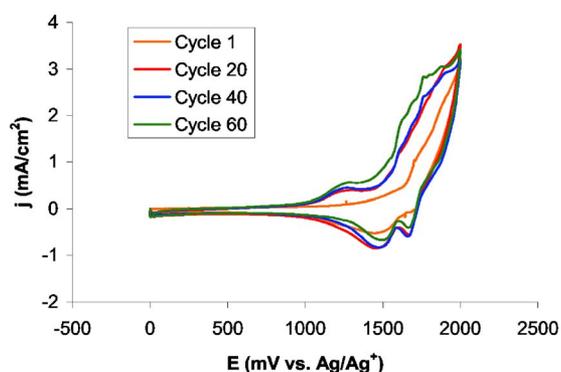
Figure 3. (Color online) Voltammograms generated by repeated cycling of applied potential at 30 mV/s during electropolymerization of DTDMPy.

Figure 5. (Color online) Redox cycling of poly(DTDMPy) produced with a narrow potential scan. Faint n-doping signals may be due to lack of cycling at n-doping potentials during polymerization.

oxidized, giving a radical cation in which the radical is located upon the 5-position of the terminal thiophene. This situation of course gives rise to the desired polymer. On the other hand, the radical may migrate to the 3-position of the pyrazole ring so that the positive charge resides upon the nitrogen at the 1-position of the ring. In this case, the steric hindrance around the radical center most likely prevents any coupling. As the applied potential becomes more negative, the stabilized radical cations are then reduced without coupling. It seems that the resonance form of the radical cation in which the radical is located at the 3-position of the pyrazole ring and the positive charge is found on the nitrogen is the more prevalent structure, as the monomer redox couple is much more intense in the voltammograms than are the current responses corresponding to the polymer.

Upon cycling of the polymer film in monomer-free 100 mM TMABF$_4$/propylene carbonate, a redox couple with an onset of about 1500 mV and peak ca. 1800 mV is readily observed (Fig. 5). The rather positive potentials required to oxidize this polymer are most likely a result of the electron-deficient pyrazole units in the polymer backbone. In addition to the p-doping signals, less intense current responses can be observed at more negative potentials, suggesting that the polymer is being n-doped to some degree. The relative difference in intensity between the p-doping and n-doping regions of the voltammograms may be a result of the electrodeposition process. As the applied potential is cycled between 0 and 2000 mV to deposit polymer, ions necessarily migrate between the growing polymer film and the electrolyte solution during the oxidation and reneutralization processes. This process establishes channels for ions to maintain charge balance during postdeposition cycling. Because ion channels appropriate for p-doping are established during film growth at positive potentials, the process of p-doping proceeds quite well. On the other hand, during polymer n-doping, the ion transport process is probably quite different, and the appropriate channels for
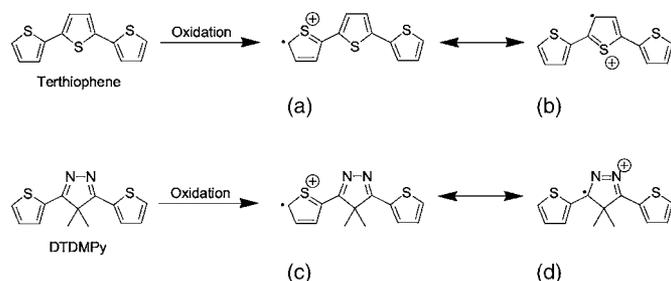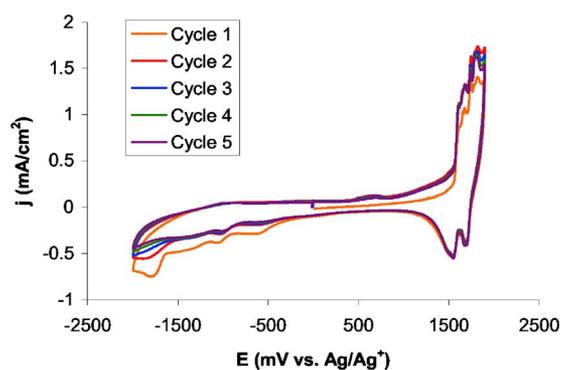
ion movement have not been established. To establish these channels, it may be necessary to cycle to n-doping potentials during electropolymerization.

In order to determine the effects of a broader cycling window, a new film was deposited by cycling the applied potential between −2000 and 2000 mV. As observed previously with electrodeposition scans between 0 and 2000 mV, the oxidative region of the voltammograms shows oxidations corresponding to the monomer at about 1500 mV and the polymer at roughly 1200 mV (Fig. 6). In addition, there is a faint n-doping process that can be discerned at roughly −1200 mV. The voltammograms from this electropolymerization suggest that both anions and cations are moving into and out of the film during the deposition. Electrochemical quartz crystal microbalance experiments are planned to explore the ion transport process in more detail.

The material was cycled from −2 to +2 V at 25, 50, and 100 mV per second. The coulombic efficiency of the 100 mV/s scan was markedly lower than those of the 25 and 50 mV/s scans. Furthermore, the 100 mV/s scan lacked the peak structure of the lower scan rates, particularly during the reoxidation, which peaks at approximately −0.8 V.

Cycling of the polymer films in monomer-free electrolyte solution gave several interesting results (Fig. 7). First, during the initial cycles between 2.0 and −2.0 V, the material seems to show very little electroactivity at all. However, the voltammograms change significantly over 50 cycles before stabilizing. Initially, the polymer oxidation onset at 1200 mV is not accompanied by a peak that could be attributed to reduction of the polymer to the neutral state. The polymer oxidation gradually becomes more prominent with extended cycling, and a reductive current response centered at 200 mV

Figure 4. Oxidation of terthiophene showing structures giving rise to (a) desirable 2,5-linkages and (b) often-undesirable 3,5-linkages; oxidation of DTDMPy showing structures leading to (c) polymer and (d) monomer reneutralization.
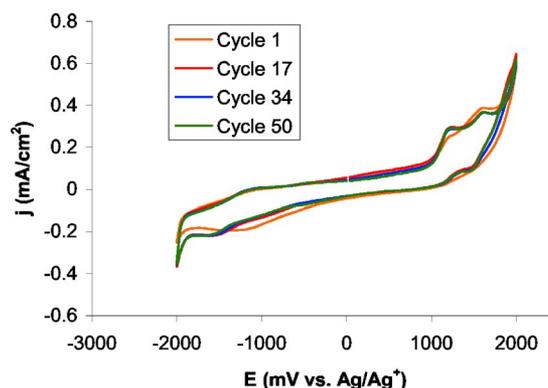

Figure 6. (Color online) Electrodeposition of poly(DTDMPy) at 30 mV/s with an expanded potential scan range to include n-doping potentials.
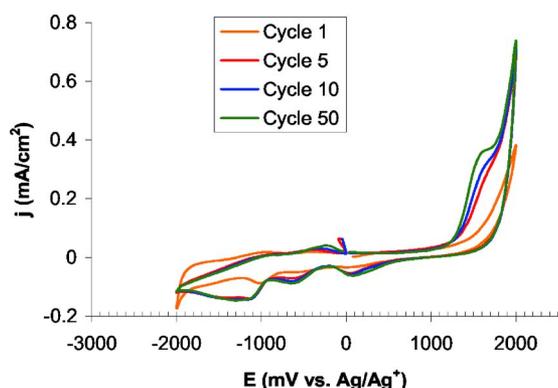
Figure 7. (Color online) Cycling of poly(DTDMPy) film produced with an expanded potential scan. Current responses corresponding to n-doping are more prominent and peak separation of the p-doping redox couple is considerably increased as compared to films with a relatively narrow voltage window.

Figure 8. (Color online) Voltammograms of poly(DTDMPy) films indicating that oxidation with an onset of 1200 and reduction centered at 200 mV are coupled.

gradually develops. At the same time, more prominent current responses at relatively negative potentials gradually become more intense. Negative current responses at −700 and −1300 mV are attributable to reduction of the neutral polymer to the n-doped state, while positive current responses at −800 and −200 mV can be attributed to oxidation of the n-doped polymer to the neutral state. These n-doping processes are much more intense than those obtained from electropolymerization over the narrow potential window (Fig. 5). By cycling between the potentials necessary to both oxidize and reduce the polymer during deposition, ion channels were established, allowing both anions and cations to move freely from the electrolyte solution into the polymer and also to exit more easily.

The change in the voltammograms during extended cycling may be a result of trapped counterions present in the film. It is necessary to first condition the polymer films with several potential scans in order to free trapped ions and permit ion migration. However, some ion trapping may be occurring even after extended cycling. The reduction observed at about 200 mV seems to be coupled to the polymer oxidation shoulder. An initial potential scan from 800 to 2500 mV (Fig. 8) shows that the polymer film displays a shoulder on the solvent degradation signal that corresponds to polymer oxidation. However, this response is not present on successive scans, indicating that the polymer has been oxidized and remained in its oxidized state throughout the experiment. With this evidence that the two signals separated by about one volt are in fact coupled, it is possible to postulate that ion-trapping is occurring.

Conclusions

A new pyrazole-containing monomer was synthesized using an easily implemented two-step process. This material can be electropolymerized, although long cycling times are necessary to produce a film of adequate thickness for easy electrochemical characterization. The necessity for long deposition times most likely stems from a stabilization of one form of the oxidized monomer that prevents coupling and allows the monomer to be reneutralized. The
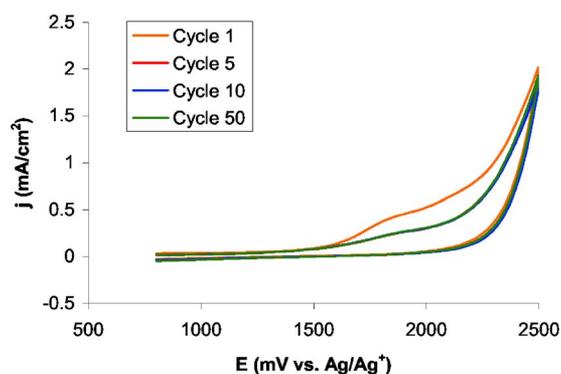
electrochemical behavior of the polymer films produced is dependent upon the conditions applied during electrodeposition. Films deposited by cycling only at relatively positive potentials show less intense n-doping responses than those obtained by scanning the applied potential throughout a wider range. However, it appears that ion trapping occurs in films produced with a wide potential window, leading to a large peak separation for the polymer's p-doping redox couple.

References

1. G. Inzelt, M. Pineri, J. W. Schultze, and M. A. Vorotyntsev, *Electrochim. Acta*, **45**, 2403 (2000).
2. J. Jagur-Grodzinski, *Polym. Adv. Technol.*, **13**, 615 (2002).
3. J. W. Schultze and H. Karabulut, *Electrochim. Acta*, **50**, 1739 (2005).
4. D. M. de Leeuw, M. M. J. Simenon, A. R. Brown, and R. E. F. Einerhand, *Synth. Met.*, **87**, 53 (1997).
5. K. Wilbourn and R. W. Murray, *Macromolecules*, **21**, 89 (1988).
6. M. Quinto, S. A. Jenekhe, and A. J. Bard, *Chem. Mater.*, **13**, 2824 (2001).
7. A. Rudge, J. Davey, I. Raistrick, S. Gottesfeld, and J. P. Ferraris, *J. Power Sources*, **47**, 89 (1994).
8. A. Berlin, G. Zotti, S. Zecchin, G. Schiavon, B. Vercelli, and A. Zanelli, *Chem. Mater.*, **16**, 3667 (2004).
9. D. J. Irvin, C. J. DuBois, and J. R. Reynolds, *Chem. Commun. (Cambridge)*, **1999**, 2121 (1999).
10. P. J. Skabara, I. M. Serebryakov, I. F. Perepichka, N. S. Sariciftci, H. Neugebauer, and A. Cravino, *Macromolecules*, **34**, 2232 (2001).
11. H.-F. Lu, H. S. O. Chan, and S.-C. Ng, *Macromolecules*, **36**, 1543 (2003).
12. A. P. Kulkarni, C. J. Tonzola, A. Babel, and S. A. Jenekhe, *Chem. Mater.*, **16**, 4556 (2004).
13. G. Brocks and A. Tol, *Synth. Met.*, **101**, 516 (1999).
14. G. P. Evans, in *Advances in Electrochemical Science and Engineering*, H. Gerischer and C. W. Tobias, Editors, p. 1, VCH Publishers, Inc., New York (1990).